

EFFECT OF DOPANT AND DOPANT TO CATALYST MOLAR RATIO IN THE VISIBLE LIGHT PHOTOCATALYSIS OF GASEOUS FORMALDEHYDE USING A SYNTHESIZED MULTI-ELEMENT DOPED TITANIUM DIOXIDE

LACISTE M., LIN Y.T., DE LUNA M.D. and LU M.C.

E-mail: maxiethecat2@yahoo.com

ABSTRACT

A multi-element doped TiO₂ photocatalyst was synthesized using sol-gel method to develop a novel photocatalyst for the degradation of gaseous formaldehyde under visible light. Varying molar ratios (mol% in TiO₂) from 0 to 5% of ammonium fluoride, silver nitrate, and sodium tungstate as dopant precursors for nitrogen, fluorine, silver and tungsten were used. Photodegradation of gaseous formaldehyde was examined using immobilized photocatalysts on glass tubular reactors illuminated with blue LEDs. The photocatalytic yield is analyzed based on photocatalyst surface properties from X-ray photoelectron spectroscopy (XPS), Fourier Transform Infrared (FTIR) spectrophotometry and X-ray Diffraction (XRD) characterization results. The modifications applied enhanced the visible light capability of the catalyst compared to the undoped catalyst and Degussa P-25.

1. Introduction

Any photocatalyst with poor visible-light activity can be modified with metal or non-metal elements to be active under visible-light irradiation. Metal ions act as electron-hole pair capture traps, hence inhibiting recombination occurrence and widen the available wavelength range, consequently increasing the utilization rate of visible light (Wilke & Breuer, 1999). Metal atoms can suppress the recombination of photo-induced electron-hole pairs thereby increasing the photocatalytic efficiency (Zhang & Liu, 2008). Non-metal atoms as dopants can incorporate in the lattice structure of titanium dioxide and create mid-gap states thereby decreasing the band gap and increasing visible light photocatalytic response (Zhang & Liu, 2008).

In this study, tungsten [W], silver [Ag], nitrogen [N], and fluorine [F] doping is examined.

W-doping is found to significantly improve the visible-light photoactivity of TiO₂. A sol-gel synthesized 0.5 percent W doped titanium dioxide under blue light irradiation showed photocatalytic activity equal to 74 percent of the commercial Degussa P-25 under UV irradiation (Putta, Lu, & Anotai, 2011).

Silver nanoparticles on TiO₂ surface enhance the charge separation of electron holes by acting as electron acceptors (Barakat, Kanjwal, Al-Deyab, Chronakis, & Kim, 2011). Page et. al. reported that the presence of the silver oxide Ag₂O in conjunction with titania marked an increased photocatalytic activity due to stabilization of photogenerated electron-hole pairs at the titania surface by localization of the photogenerated electron onto the silver oxide (Page, Palgrave, Parkin, Wilson, Savin, & Chadwick, 2007).

Ananpattarachai et. al. studied substitutional and interstitial N-doping into the TiO₂ structure and reported that nitrogen dopants effectively extended absorption of TiO₂ into the visible light range (Ananpattarachai, Kajitvichyanukul, & Seraphin, 2009). A narrowed band gap will facilitate excitation of electrons from the valence band to the conduction band in the modified titania catalyst under visible light illumination, which can result in higher photocatalytic activities.

Li et. al. reported that several beneficial effects including enhancement of surface acidity, creation of oxygen vacancies, and increased active sites are attributed to F-doped titania in the degradation of gas-phase acetaldehyde (Li, Haneda, Hishita, Ohashi, & Labhsetwar, 2005).

The high electronegativity of fluorine could stabilize the electron release upon oxygen depletion during calcination treatment and making visible light photocatalytic excitation by extrinsic absorption bands of the generated oxygen vacancies generate free charge carriers that can take part in surface chemical reactions (Dozzi, Ohtani, & Selli, 2011).

2. Materials and methods

All chemicals used were analytical grade. Tetra-n-butyl orthotitanate [C₁₆H₃₈O₄Ti] MW= 340.32 g/mol (98%, Merck, KGaA, Darmstadt Germany) was the titanium dioxide precursor. Ammonium fluoride (NH₄F) MW = 37.037 g/mol (99%, Ferak GMBH, West Berlin), silver nitrate (AgNO₃) MW= 169.87 g/mol (99.8%, Ferak GMBH, West Berlin) and, sodium tungstate dihydrate (Na₂WO₄·2H₂O) MW= 329.86 g/mol (99%, Ferak GMBH, West Berlin) were used as dopants. Deionized (DI) water with resistivity value of 18.2 MΩ cm was used for dilution and washing.

Varying amounts of the dopants (0, 0.2, 0.35, 0.7, 1.4, 2 mol% in TiO₂) were used during synthesis. The synthesis method used is based on a modified sol-gel method (Tolosa, Lu, Mendoza, & Rollon, 2011).

The physical and structural properties of the different photocatalyst were checked using a Siemens Kristalloflex 760 X-ray Diffraction (XRD) spectrophotometer. Surface compositions were determined using ULVAC- PHI 5000 Versa Probe X-ray Photoelectron Spectrometer (XPS) and functional groups were analyzed using a JASCO FT-IR 4100 Fourier Transform Infra-red (FTIR) spectrophotometer. Table 1 shows the formulations for each synthesized photocatalysts used in this study.

Table 1: Synthesized photocatalyst formulations

Photocatalyst ID	Ag (mol%)	F (mol%)	N (mol%)	W (mol%)
U35	0	0	0	0
Ay35	0.7	0	0	0
Fy35	0	0.7	0	0
Ny35	0	0	1.4	0
Wy35	0	0	0	0.2
Cx35	0.35	0.35	0.7	0.1
Cy35	0.7	0.7	1.4	0.2
Cz35	1.0	1.0	2.0	0.3

3. Results and discussion

3.1. Effect of individual dopant

The HCHO removal plots in Figure 1 for the modified titanium dioxide photocatalysts show that the removal of gaseous formaldehyde with illumination (Adsorption + Photocatalysis) is greater than the removal due to adsorption only. This means that the doped synthesized photocatalysts are photoactive under visible light. The plot also show that adsorption determines extent of degradation, i.e. low adsorption results to low degradation and high adsorption results to high degradation. Photocatalyst Cy35 exhibits the highest adsorption of 41% after 2 hours in the dark and consequently gave the highest degradation of 88.1% after 2 hours of illumination.

The plot in Figure 1 shows addition of silver nitrate has the greatest effect on the degradation of gaseous formaldehyde. However, performance of the combined multi-element doped titanium dioxide (Cy35) showed the highest removal exhibiting a 4 percent edge over the AgNO₃-doped photocatalyst (Ay35). The performance of the individual dopant precursor increases in the order of N < F/N < W < Ag/N < Ag/F/N/W.

Comparison between adsorption (dark reaction) and photocatalytic reaction using the different synthesized photocatalysts i.e., C/Co(adsorption) – C/Co(photocatalysis) after two hours gives a

trend similar to the XRD crystallinity trend observed in Figure 2 *i.e.*, Wy35 gives the highest photocatalytic potential with 57 percent increase in gaseous formaldehyde degradation and Cy35 photocatalyst exhibited a 47 percent photocatalytic potential.

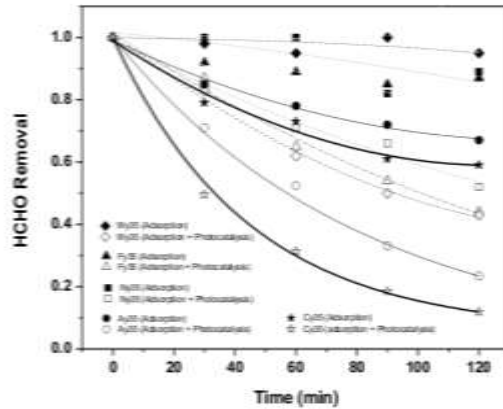


Figure 1: Effect of individual dopant precursor on photocatalytic rate. Experimental Conditions: 0.1g/L catalyst, 2ppm initial formaldehyde concentration, 30C, 25.7 W/m²

The XRD plot in Figure 2 shows decreasing crystallinity in the order of Wy35 > Cy35 > Ay35 > Ny35 > Fy35. Increased crystallinity is associated with increase photocatalytic activity.

Figure 3 shows the O1s peaks of each synthesized photocatalyst doped with individual dopant precursors. The O1s peak shifts to decreasing binding energy values following the trend, U35 > Wy35 > Ay35 > Fy35 > Cy35 > Ny35 (529.8563 eV > 529.7598 eV > 529.7322 eV > 529.6656 eV > 529.6333 eV > 529.5219 eV). This shift in binding energies from higher to lower values is a consequence of an increase in screening by additional electrons in the system suggesting a red shift due to the creation of mid band gap states. The Fy35 synthesized photocatalyst uniquely exhibits a spin orbital splitting with additional peaks at 532.0656 eV and 533.2656 eV. This is in agreement with a similar study on titanium dioxide-fluorine doped tin oxides (Kronawitter, *et al.*, 2012). Kronawitter, *et. al.* indicated that the unique peak come from the hybridization of unoccupied Ti d(t_{2g}) levels with O 2p levels, which exist in the conduction bands of titanium oxides.

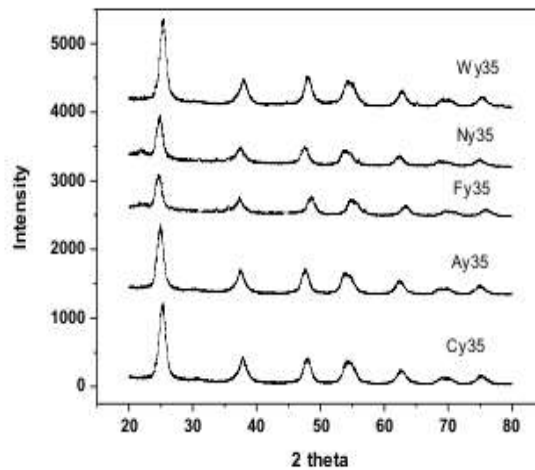


Figure 2: XRD spectra of synthesized photocatalysts doped with individual dopant precursor

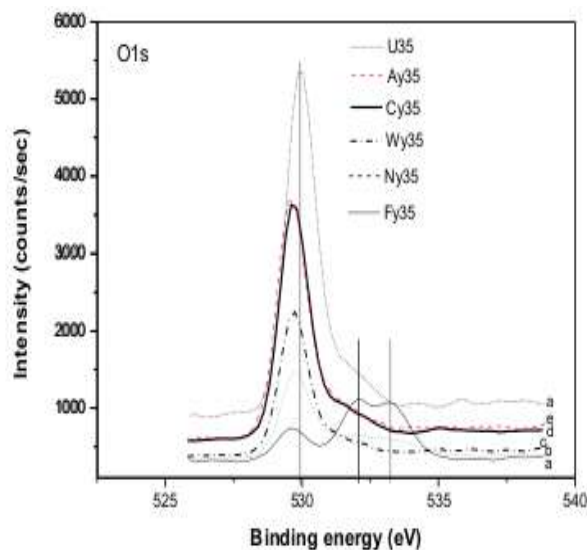


Figure 3: O1s XPS spectra of the different dopant used in the synthesized photocatalyst, a. Fy35, b.Ny35, c. Wy35, d.Cy35 e. Ay35, f. U35

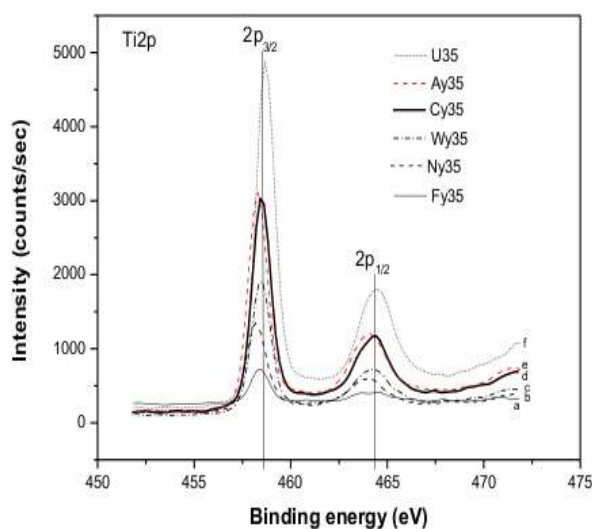


Figure 4: Ti2p XPS spectra of the different dopant used in the synthesized photocatalyst, a. Fy35, b. Ny35, c. Wy35, d.Cy35, e.Ay35, f. U35

The Ti2p_{3/2} binding energies shown in Figure 4 for the synthesized photocatalysts follow a trend, U35 > Wy35 > Fy35 > Cy35 > Ay35 > Ny35 (458.66 eV > 458.56 eV > 458.47 eV > 458.43 eV > 458.33 eV > 458.3219 eV).

On the other hand, the intensity of the peaks is related to the concentration of titanium within the sample. It is observed that the peak intensities vary according to the trend; Fy35 < Ny35 < Wy35 < Cy35 < Ay35 < U35.

3.2. Effect of dopant molar concentration

Figure 5 presents the residual formaldehyde plot of synthesized photocatalysts with varying dopant molar concentrations. The adsorption and photocatalysis trends are similar suggesting that the photoactive sites increase with the amount of dopant. The optimum dopant molar concentration is

0.7%Ag/0.7%F/1.4%N/0.2%W calcined at 300 0C for five hours (Cy35) resulting to a formaldehyde photocatalytic degradation of 88.1%.

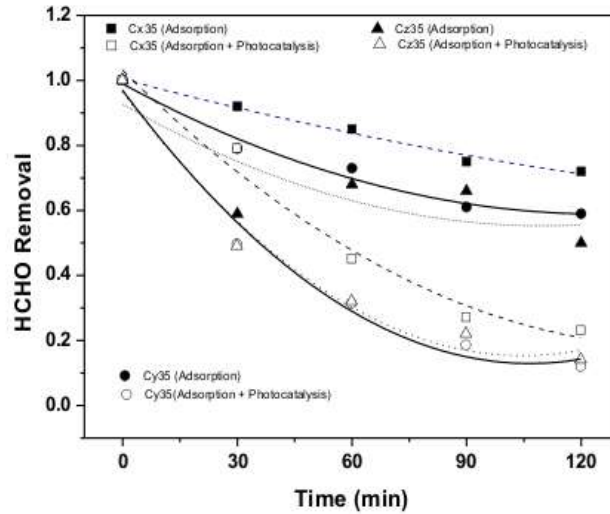


Figure 5: Residual formaldehyde plot using synthesized photocatalysts with varying dopant molar concentrations. 0.1 g/L photocatalyst, 2ppm formaldehyde, 30 0C, Adsorption (0 W/m²), Photocatalysis (Vertical 10W/m² / Horizontal 25W/m²).

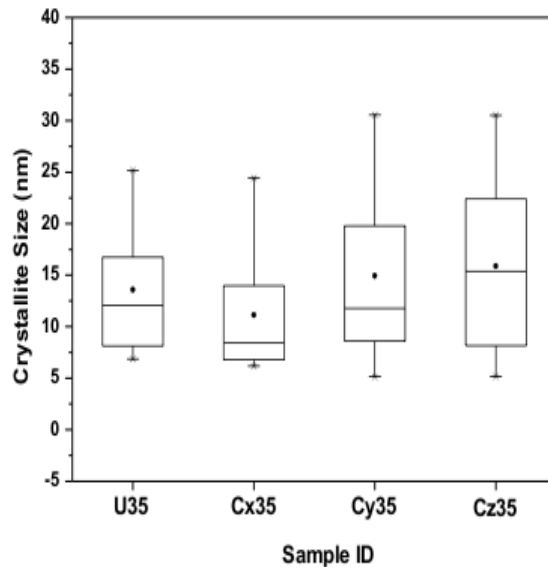


Figure 6: Comparison of crystallite sizes of synthesized photocatalysts doped with different dopant molar concentrations

4. Conclusion

The gaseous formaldehyde photocatalytic degradation plots using the photocatalysts doped with varying amounts of the dopant shows that adsorption increases with the amount of dopant within the molar concentration used.

As for the photocatalysis part, Cy35 gave the highest photocatalytic degradation at 88.1 % followed by Cz35 resulting to a formaldehyde photocatalytic degradation of 86%.

To elucidate the results of the photocatalytic degradation experiments, XRD results of the photocatalysts are analyzed. Comparison of crystallite sizes of the synthesized photocatalyst with different molar concentrations of silver, fluorine, nitrogen and tungsten shows that the mean crystallite size increases as the amount of dopant is increased, however the spread of the box which describes the spread of the values indicates a greater variability and may indicate increased amount of defects in the crystal lattice of the photocatalyst.

Adsorption of gaseous formaldehyde follows the same trend as the crystallite size of the synthesized photocatalyst presumably because as the crystallite size increases the number of available functional groups available for the formaldehyde to attach to increases as well.

The hydroxyl group at 1630-1660 per cm shows greatest wave number for the Cy35 synthesized photocatalyst. Wave numbers is related to the strength of the bonds that hold the functional group on the surface. Since for all the synthesis parameters varied, Cy35 has the largest wave number and consequently the strongest hydroxyl bonded on the surface of the photocatalyst, it is presumed that this is one of the reason for the high photocatalytic degradation of gaseous formaldehyde using the same photocatalyst giving a removal of 88.1%.

REFERENCES

1. Ananpattarachai, J., Kajitvichyanukul, P., & Seraphin, S. (2009), Visible light absorption ability and photocatalytic oxidatin activity of various interstitial N-doped TiO₂ prepared from different dopants. *Journal of Hazardous Materials* 169, 253-261.
2. Barakat, N., Kanjwal, M., Al-Deyab, S., Chronakis, I., & Kim, H. (2011), Influences of Silver-Doping on the Crystal Structure, Morphology and Photocatalytic Activity of TiO₂ Nanofibers. *Materials Sciences and Applications* 2, 1198-1193.
3. Dozzi, M., Ohtani, B., & Sellì, E. (2011), Absorption and action spectra analysis of ammonium fluoride-doped titania photocatalysis. *Physical Chemistry Chemical. Physics.* 13 , 18217-18227.
4. Li, D., Haneda, H., Hishita, S., Ohashi, N., & Labhsetwar, N. (2005), Fluorine-doped TiO₂ powders prepared by spray pyrolysis and their improved photocatalytic activity for decomposition of gas-phase acetaldehyde. *Journal of Fluorine Chemistry* 126 , 69-77.
5. Page, K., Palgrave, R., Parkin, I., Wilson, M., Savin, S., & Chadwick, A. (2007), Titania and silver-titania composite films on glass potent microbial coatings. *Journal of Materials Chemistry* 17 , 95-104.
6. Putta, T., Lu, M., & Anotai, J. (2011). Photocatalytic activity of tungsten-doped TiO₂ with hydrothermal treatment under blue light irradiation. *Journal of Environmental Management* 92 , 2272-2276.
7. Tolosa, N. S., Lu, M. C., Mendoza, H. D., & Rollon, A. P. (2011),The effect of the composition of tri-elemental doping (K, Al, S) on the photocatalytic performance of synthesized TiO₂ nanoparticles in oxidizing 2-chlorophenol over visible light illumination. *Applied Catalysis A: General* 401 , 233-238.
8. Vasconcelos, D., Costa, V., Nunes, E., Sabioni, A., Gasparon, M., & Vasconcelos, W. (2011), Infrared spectroscopy of titania sol-gel coatings on 316L stainless steel . *Materials Sciences and Applications* 2 , 1375-1382.
9. Wilke, K., & Breuer, H. D. (1999), The influence of transition metal doping on the physical and photocatalytic properties of titania. *Journal of Photochemistry and Photobiology, A* 121 (1) , 49-53.
10. Y. Zhang, Y. W. (2011), Photocatalytic degradation of phenanthrene in nonionic-anionic surfactant using titania catalyst. *Scientific Research and Essays* 6(30), 6372-6381.
11. Zhang, X., & Liu, Q. (2008), Visible-light-induced degradation of formaldehyde over titania photocatalyst co-doped with nitrogen and nickel. *Applied Surface Science* 254 , 4780–4785.